Office of Air Force Research

Grant AF-AFOSR 1226-67

Technical Report No. 1

DYNAMIC SNAP-THROUGH OF IMPERFECT VISCOELASTIC SHALLOW ARCHES

by

N. C. Huang and W. Nachbar

Department of the Aerospace and Mechanical Engineering Sciences
UNIVERSITY OF CALIFORNIA, SAN DIEGO
La Jolla, California

March 1967

DYNAMIC SNAP-THROUGH OF IMPERFECT VISCOELASTIC SHALLOW ARCHES[1]

N. C. Huang[2] and W. Nachbar[3]

ABSTRACT

Dynamic snap-through or dynamic buckling of imperfect viscoelastic shallow arches with hinged ends is considered under step loads of infinite duration. Attention is principally devoted to the influence both of small imperfections and of small amounts of damping, acting together, on the critical loads. For the problem considered, the Voigt model is used for viscoelasticity, the deflection is represented by the first two harmonic modes, and imperfections have the shape of the second (antisymmetric) mode. Results obtained by numerical integration of the differential equations show that the critical load exhibits a jump discontinuity in the limit both for vanishing imperfection and for vanishing viscosity. Critical loads for slight imperfect and elastic (inviscid) arches are slightly higher than those from the saddle point formula of Hoff and Bruce (J. Math. Physics, 32, 1954, 276), confirming that the formula gives a lower bound on the critical load. However, critical loads for arches with slight imperfection and slight viscosity are considerably higher than for the elastic arches. Another closed-form expression is shown to be in good agreement with these results. For finite amounts of viscosity, the critical loads tend rapidly to the values obtained for infinite viscosity, which are the same as the critical loads for quasi-static buckling. Apart from the jump discontinuity at zero, the critical load for any viscosity decreases continuously and monotonically with imperfection.

[1] Research sponsored by the Air Force Office of Scientific Research, Office of Aerospace Research, United States Air Force under AFOSR Grant AF-AFOSR 1226-67.

[2] Assistant Professor
[3] Professor

Department of the Aerospace and Mechanical Engineering Sciences, University of California, San Diego, La Jolla, California

Nomenclature

A	cross section area
a_n	Eq. (10)
$b_n(t)$	Eq. (11)
D	total energy dissipation, Eq. (26)
E	Young's modulus
E_o	effective spring constant for Voigt solid
f_n	Eq. (12)
H	horizontal thrust
I	moment of inertia of cross section of arch
K	kinetic energy, Eq. (25)
L	span of arch
M	bending moment
M_1, M_2	local minima - see discussion above Eq. (40)
n	any positive integer
$q(x)$	load on arch
R_n	Eq. (15)
r	$\equiv R_1$, load parameter
r_c	minimum load for snap-through
r_{cg}	Eq. (49)
r_{cm}	critical load of Hoff and Bruce, Eq. (43)

r_{cp}	perfect arch dynamic snap-through load, Eq. (32)
r_{cs}	quasi-static snap-through - see last column of Table 3
t	time
U	potential energy, Eq. (24)
U_e	potential energy at critical point
V	vertical shear
$w(x, t)$	deflection
$w_o(x)$	initial deflection
x	horizontal coordinate
$y(t)$	$\equiv b_1(t)$; first harmonic of deflection
y_o	$\equiv y(0)$: rise of arch
y_e	value of y at critical point
y_{c1}, y_{c2}	critical values of y_e; Eqs. (47a, b)
$z(t)$	$\equiv b_2(t)$; second harmonic of deflection
z_o	$\equiv z(0)$: imperfection amplitude
z_e	value of z at critical point
Δ	approximate shortening of arch length, Eq. (5)
η	effective viscosity for Voigt solid
$\varkappa$	nondimensional viscosity, Eq. (15)
ρ	mass of arch per unit length
τ	nondimensional time, Eq. (15)

1. INTRODUCTION

In this paper, the dynamic snap-through or dynamic buckling behavior of imperfect viscoelastic shallow arches under a suddenly applied load of infinite duration is considered. The critical load is defined as the smallest magnitude of load under which the arch can deform to a snapped-through position.

The problem of the dynamic buckling of sinusoidal elastic shallow arches has been studied by Hoff and Bruce [1][4] and by Simitses [2] with analyses based upon the behavior of the trajectories describing the motion on the potential surface. Since small geometric imperfections, or small disturbing loads or initial velocities, affect the shape of the potential surface only to the second order in small quantities, it is possible to include the effects of such perturbations by an analysis based upon the potential surface for the perfect structure. This analysis for the arch shows that, if the arch is not very flat, the critical load of a perfect arch having the shape of $\sin x$ will be associated with an asymmetric buckling mode shape $\sin 2x$. This critical load is obtained from the condition that it is possible for a trajectory

---

[4] Numbers in brackets designate references at the end of the paper.

to reach a saddle point on the potential surface. The critical load is that load for which the potential energy at the saddle point becomes equal to the total energy.

Several reasonable objections have been raised to this potential surface method of analysis. One objection is that the method is limited to problems with a small number of degrees of freedom. The arguments used in the potential surface method are essentially geometric, and it is much more difficult to deal with the hyper-surfaces that are encountered if more than two degrees of freedom are considered. We will not attempt in this paper to generalize this method of analysis but will, in fact, confine our discussion to a specific system with two degrees of freedom where the method has already proven feasible.

Another objection, and the one to which the major attention of this paper will be devoted, is that the saddle point criteria does not assure that the solution to the differential equations, with its initial conditions, does indeed have a trajectory on the potential energy surface which goes into the saddle point at the critical load. Hoff and Bruce pointed to this deficiency in the following statement of their paper regarding the critical value of their load parameter Q, ([1], pp. 284-5): "If Q has this value one can say that it is <u>possible</u> for the initially

disturbed system to be displaced to the stable 'buckled' equilibrium configuration, $(0, e z_s)$, if it follows the appropriate path on the energy surface." We have underlined the words possible and if. The significance of these words is amplified in the work done in [2], where the Hoff and Bruce critical load is not regarded as a rigorous critical load but as a lower bound or minimum possible critical load for dynamic snap-through of the arch.

The question then arises: if the saddle point critical load is a lower bound on the true critical load, how good an approximation to the critical load is it? To investigate this question, it is necessary to integrate the governing differential equations, to look for the minimum load at which the solution exhibits snap-through, and to compare this minimum load with the predictions of the potential surface analysis. In carrying out this program, we cannot confine ourselves to perfect arches of sinusoidal shape. Indeed, it is readily seen that if the differential equations and subsidiary conditions are symmetric, then the solutions obtained will be symmetric, and the trajectories of these solutions could never approach a saddle point that is associated with an unsymmetrical mode. It is necessary then to consider imperfections or, at the least, to consider the limiting behavior of an imperfect arch as the amplitude of the imperfections tends towards zero. A more elaborate analysis [2] has already indicated that second harmonic (or

first antisymmetric) imperfections will have the greatest effect on the critical load and so, in the present paper, only the first and second harmonics are considered to describe the initial shape and subsequent deformation of the arch.

Viscoelasticity is introduced here because it is a more realistic material description for dynamic problems than the assumption of ideal elasticity, and also because it often makes the analysis less ambiguous, as is illustrated by our study of dynamic buckling of a single degree-of-freedom structure [3]. Perhaps more important, however, is that we want to see whether the critical loads obtained for the viscoelastic material in the limit as the viscosity parameter tends to zero are the same as the critical loads obtained under the same conditions for the elastic material in which the viscosity is equal to zero. In the case of imperfections we already know that the limit of the critical load for vanishing imperfections may not be equal to the critical load for zero imperfections. We then may have a jump between the limiting value and the value at zero. We want to see whether such a jump is exhibited also with respect to the viscosity parameter.

We will also present, in addition to the investigations already described, results on the effects of finite imperfections and finite viscosity on the critical load. In this paper, we will discuss all these questions only with regard to the following problem: the

arch is considered hinged at both ends; the loading is sinusoidal in shape, and is of constant magnitude and infinite duration in time; the material of the arch is considered to be a Voigt solid.

2. BASIC EQUATIONS

Consider a shallow arch of span L, as shown in Fig. 1. The cross section of the arch is assumed to be uniform along the span, with cross-sectional area A and moment of inertia I about the central axis. The load $q(x)$ per unit length is suddenly applied at zero time and maintained at constant magnitude thereafter. At time t, the central axis of the arch, having original height $w_o(x)$, is deformed to a height $w(x, t)$. With use of d'Alembert's principle, the dynamic load is $q(x) + \rho \frac{\partial^2 w}{\partial t^2}$ positive in the $-w$ direction, as shown in Fig. 2, where ρ is the mass of the arch per unit length. If we denote the horizontal thrust, vertical shear and bending moment by H, V and M, respectively, the equations of equilibrium can be obtained directly from Fig. 2:

$$V' = -(q + \rho \ddot{w}) \tag{1}$$

and

$$M' = V - Hw' \quad , \tag{2}$$

where $(\,)' \equiv \frac{\partial}{\partial x}(\,)$ and $(\dot{}) \equiv \frac{\partial}{\partial t}(\,)$.

If the arch is elastic, the Euler-Bernoulli assumption gives

$$M = EI(w'' - w_o'') \tag{3}$$

where E is Young's modulus. From Eqs. (1), (2) and (3) the following equation is obtained:

$$EI(w'''' - w_o'''') + Hw'' + q + \rho\ddot{w} = 0 \quad . \tag{4}$$

For shallow arches, the shortening of the length of the arch during deformation can be written approximately as

$$\Delta = \frac{1}{2}\int_o^L \left[\left(w_o'\right)^2 - \left(w'\right)^2 \right] dx \quad , \tag{5}$$

and the horizontal thrust H can be expressed approximately as a constant, viz.

$$H = \frac{AE\Delta}{L} \quad . \tag{6}$$

From Eqs. (4), (5) and (6), we then obtain

$$EI\left(w'''' - w_o''''\right) + w''\frac{A}{2L}E\int_o^L \left[\left(w_o'\right)^2 - \left(w'\right)^2 \right] dx + q + \rho\ddot{w} = 0 . \tag{7}$$

For an arch with both ends hinged, the deflection and the bending moments at the ends must vanish. The boundary conditions are:

$$w_o(0) = w_o(L) = w(0,t) = w(L,t) = 0 \quad , \tag{8}$$

and

$$w''(0,t) = w_o''(0) \; ; \quad w''(L,t) = w_o''(L) \quad . \tag{9}$$

These conditions are satisfied termwise if we put

$$w_o(x) = 2\left(\frac{I}{A}\right)^{1/2} \sum_{n=1}^{\infty} a_n \sin\frac{n\pi x}{L} \tag{10}$$

and

$$w(x, t) = 2\left(\frac{I}{A}\right)^{1/2} \sum_{n=1}^{\infty} b_n(t) \sin \frac{n\pi x}{L} \tag{11}$$

where the deflections have been normalized with respect to the radius of gyration $(I/A)^{1/2}$, so that the constants a_n and the functions $b_n(t)$ are dimensionless. Further, let the load intensity be represented by

$$q(x) = \sum_{n=1}^{\infty} f_n \sin \frac{n\pi x}{L} \quad . \tag{12}$$

Substituting Eqs. (10), (11) and (12) into Eq. (7), we obtain

$$n^4 E(b_n - a_n) + n^2 b_n E \sum_{j=1}^{\infty} [j^2(b_j^2 - a_j^2)] + \frac{L^4}{2\pi^4 I}\left[\left(\frac{A}{I}\right)^{1/2} f_n + 2\rho \ddot{b}_n\right] = 0$$

$$\text{for } n = 1, 2, \ldots \quad . \tag{13}$$

We shall use the Voigt model to represent the viscoelastic property of the arch. The elastic constant E in Eq. (13) is therefore replaced by the differential operator $E_o + \eta \frac{\partial}{\partial t}$, where E_o is the effective spring constant and η is the effective viscosity of the material. Consequently, Eq. (13) becomes

$$n^4\left(E_o + \eta \frac{\partial}{\partial t}\right)\left(b_n - a_n\right) + n^2 b_n \left(E_o + \eta \frac{\partial}{\partial t}\right) \sum_{j=1}^{\infty}\left[j^2\left(b_j^2 - a_j^2\right)\right]$$

$$+ \frac{L^4}{2\pi^4 I}\left[\left(\frac{A}{I}\right)^{1/2} f_n + 2\rho \ddot{b}_n\right] = 0$$

$$\text{for } n = 1, 2, \ldots \quad . \tag{14}$$

Let us introduce the following dimensionless quantities

and notation:

$$R_n = \frac{L^4}{2\pi^4 E_o I}\left(\frac{A}{I}\right)^{1/2} f_n \ , \quad \tau = \frac{\pi^2}{L^2}\left(\frac{E_o I}{\rho}\right)^{1/2} t \ ,$$

$$\varkappa = \eta \frac{\pi^2}{L^2}\left(\frac{I}{E_o \rho}\right)^{1/2} \quad \text{and} \quad (\dot{}) \equiv \frac{\partial}{\partial \tau}(\,) \ . \tag{15}$$

Equation (14) becomes

$$n^4\left(1 + \varkappa \frac{\partial}{\partial \tau}\right)(b_n - a_n) + n^2 b_n\left(1 + \varkappa \frac{\partial}{\partial \tau}\right)\sum_{j=1}^{\infty}\left[j^2\left(b_j^2 - a_j^2\right)\right] + \\ + R_n + \ddot{b}_n = 0$$

$$\text{for } n = 1, 2, \ldots \ . \tag{16}$$

We shall assume that the load distribution is sinusoidal and consider only the first and second harmonics for the initial and the deformed shapes of the arch, i.e.:

$$a_n = b_n = 0 \quad \text{for } n \neq 1 \text{ or } 2 \qquad \text{and} \qquad R_n = 0 \quad \text{for } n \neq 1 \ .$$

Put $y = b_1$, $z = b_2$, $y_o = a_1$, $z_o = a_2$ and $r = R_1$. Substitution into Eq. (16) gives the governing differential equations for the motion of the arch under these constraints:

$$\ddot{y} + \varkappa\left[\left(1 + 2y^2\right)\dot{y} + 8yz\dot{z}\right] + y - y_o + y\left(y^2 - y_o^2 + 4z^2 - 4z_o^2\right) + r = 0, \tag{17}$$

and

$$\ddot{z} + 8\varkappa\left[2\left(1 + 2z^2\right)\dot{z} + yz\dot{y}\right] + 16\left(z - z_o\right) + 4z\left(y^2 - y_o^2 + 4z^2 - 4z_o^2\right) = 0 \ . \tag{18}$$

Solutions to these equations will be sought for the initial conditions:

$$y(0) = y_o, \quad z(0) = z_o, \quad \dot{y}(0) = \dot{y}_o \text{ and } \dot{z}(0) = \dot{z}_o \ . \tag{19}$$

We can, without restricting the essential problem, consider $y_o > 0$, $z_o \geq 0$ and $r \geq 0$.

The critical points of Eqs. (17) and (18) are obtained by setting $\dot{y}=\ddot{y}=\dot{z}=\ddot{z}=0$ in these equations. The critical points defined by the pairs of values (y_e, z_e) satisfy the following equations simultaneously:

$$y_e - y_o + y_e\left(y_e^2 - y_o^2 + 4z_e^2 - 4z_o^2\right) + r = 0 \ , \tag{20}$$

$$4\left(z_e - z_o\right) + z_e\left(y_e^2 - y_o^2 + 4z_e^2 - 4z_o^2\right) = 0 \ . \tag{21}$$

After z_e is eliminated from Eqs. (20) and (21), we obtain

$$\left(3y_e + y_o - r\right)^2\left[r + y_e - y_o + y_e\left(y_e^2 - y_o^2 - 4z_o^2\right)\right] + 64z_o^2 y_e^3 = 0. \tag{22}$$

The energy equation can be derived from Eqs. (17), (18) and (19) by integration and addition. It can be written as

$$U + K + D = 0 \ . \tag{23}$$

where

U = potential energy

$$= \frac{1}{2}(y - y_o)^2 + 8(z - z_o)^2 + \frac{1}{4}\left[y^2 - y_o^2 + 4(z^2 - z_o^2)\right]^2 + r(y - y_o); \tag{24}$$

K = kinetic energy

$$= \frac{1}{2}\left(\dot{y}^2 - \dot{y}_o^2\right) + \frac{1}{2}\left(\dot{z}^2 - \dot{z}_o^2\right) \quad ; \tag{25}$$

and

D = total energy dissipation

$$= \varkappa \int_o^t [\dot{y}^2 + 16\dot{z}^2 + 2(y\dot{y} + 4z\dot{z})^2]\, dt \quad . \tag{26}$$

Note that the datum of the potential surface U has been chosen so that the initial value of U is zero. Equations (20) and (21) defining the critical points of Eqs. (17) and (18) are the same as the equations $\frac{\partial U}{\partial y} = 0$ and $\frac{\partial U}{\partial z} = 0$, respectively.

3. PERFECT ARCHES WITH PERFECT INITIAL CONDITIONS ($z_o = \dot{z}_o = 0$)

From Eqs. (17), (18) and (19), we find that unsymmetric deformation of the arch can be caused by small antisymmetric initial velocities or imperfections in geometry. On the other hand, if the initial conditions are entirely symmetric, i.e., if $z_o = \dot{z}_o = 0$, we can conclude from Eq. (18) that $z(t) \equiv 0$. Therefore, under the constraints assumed above, the deformation of a perfect sinusoidal arch under perfect initial conditions remains symmetric, and the motion of the structure has only one degree of freedom which is described by $y(t)$. The differential equation and initial conditions are taken as

$$\ddot{y} + \varkappa(1 + 2y^2)\,\dot{y} + y - y_o + y^3 - y_o^2 y + r = 0 \quad . \tag{27}$$

$$y(0) = y_o \quad \text{and} \quad \dot{y}(0) = 0 \quad . \tag{28}$$

The critical points in this problem are $\dot{y} = 0$, $y = y_e$, where y_e is a root of the following cubic equation (corresponding to the roots of the square bracketed term in Eq. (22) when $z_o = 0$):

$$y_e^3 + (1 - y_o^2)\, y_e + r - y_o = 0 \quad . \tag{29}$$

Typical solutions of Eqs. (27) and (28) are shown in Fig. 3. These solutions were obtained by numerical integration (see part (b) below). For positive $\varkappa$, these curves oscillate about one of the stable equilibrium points (which are spiral points in the phase plane) with decreasing amplitudes because of continuous energy dissipation.[5] When the load parameter r passes through a critical value[6] r_c there occurs a sudden diversion of these curves from the neighborhood of one equilibrium point to the neighborhood of the other.

For problems described by a single variable, the analysis of dynamic snap-through is facilitated by the use of potential curves.

---

[5] When the value of $\varkappa$ is very small, the structure may snap back after the snap-through (see [3]).

[6] In order to be able to distinguish the critical load values obtained by numerical integration of the differential equations as opposed to closed-form expressions for r_c obtained for particular cases by use of the potential surface, we will adopt the convention of identifying the latter by special subscripts (e.g. r_{cp}, r_{cm}, r_{cg}, r_{cs}), and we will reserve the notation r_c for the former.

Equation (24) becomes

$$U = \frac{1}{2}(y - y_o)^2 + \frac{1}{4}(y^2 - y_o^2)^2 + r(y - y_o) \quad . \qquad (30)$$

Using r as a parameter, we can plot U as a function of y, as shown in Fig. 4. A discussion of the application of the potential curves for dynamic buckling analysis in a dissipative system with a single degree of freedom is given in [3]. In the following parallel discussion, snap-through, as a function of $\varkappa$, is discussed as three cases.

(a) Elastic case ($\varkappa = 0$).

No solution of Eqs. (27) and (28) can produce a positive U, in view of Eq. (23). With r increasing from zero, then, the minimum of the potential curve on the left of the U axis (Fig. 4) will not be reached by a solution until the local maximum value of U to the right of this minimum satisfies the condition $U_e \leq 0$. Therefore, the critical load can be obtained by setting the value of U equal to zero at the equilibrium point at which this maximum is attained. This gives, from Eq. (30),

$$r = \frac{1}{4}(y_o - y_e)\left[2 + (y_e + y_o)^2\right] \quad . \qquad (31)$$

By eliminating y_e between Eqs. (29) and (31), we obtain an expression for the critical load r_{cp}:

$$r_{cp} = \frac{1}{27}\left[2y_o\left(9 + 2y_o^2\right) + \left(2y_o^2 - 3\right)\left(4y_o^2 - 6\right)^{1/2}\right] \quad . \qquad (32)$$

The values of r_{cp} are plotted against y_o by one of the solid lines in Fig. 5.

From Eqs. (29) and (30), the potential energy U at all critical points is found to be

$$U_e = -\left(y_e - y_o\right)^2\left[3\left(y_e + \frac{1}{3}y_o\right)^2 + \frac{2}{3}\left(3 - 2y_o^2\right)\right] \quad . \qquad (33)$$

If y_o is less than $\frac{1}{2}(6)^{1/2} = 1.224$, Eq. (33) shows that U_e is negative at all critical points; hence, the arch always deforms to the inside-out position without snap-through.

(b) Viscoelastic case $(0 < \varkappa < \infty)$.

For the viscoelastic case, it is necessary to use numerical methods to solve the differential equation, Eq. (27), with the initial condition, Eq. (28). A Runge-Kutta-Gill method [4] has been used for this purpose. The critical load r_c is determined by the condition that the arch begins at that load to deform to the snapped-through position. The results for cases $\varkappa = 0.1$ and 0.2 are shown in Fig. 5 by solid lines.

A certain amount of energy is dissipated before the structure reaches the point of snap-through. Hence, the critical load for the viscoelastic case is higher than that in the corresponding elastic case. In the viscoelastic case, there is also a lower limit for y_o such that, for any value of y_o less than this lower limit,

the arch deforms to the inside-out position without snap-through.

(c) Quasi-static case ($\varkappa = \infty$).

The quasi-static case was first studied by Fung and Kaplan [5]. The same results are obtained here in the limit of infinite viscosity. When $\varkappa = \infty$, snap-through can occur only when the maximum of the potential curve (Eq. 30) becomes a point of inflection, i.e., at $y = y_e$, $\frac{\partial^2 U}{\partial y^2} = 0$. From this condition we have

$$y_e = \frac{(3)^{1/2}}{3}\left(y_o^2 - 1\right)^{1/2} \quad . \tag{34}$$

The quasi-static critical load r_{cs} can then be derived from Eqs. (29) and (34):

$$r_{cs} = y_o + \frac{2}{9}(3)^{1/2}\left(y_o^2 - 1\right)^{3/2} \quad . \tag{35}$$

In Fig. 5, r_{cs} is plotted against y_o by a solid line. Note that when $y_o < 1$, there cannot be a point of inflection on the potential curve, Hence, for $y_o < 1$, the arch will deform to an inside-out position under any positive load.

4. ARCHES WITH INFINITESIMAL GEOMETRIC IMPERFECTION ($z_o = 0^+$)

The perfect arch discussed in the last section is an overly idealized model. It is known that the critical load may change drastically due to the effect of small geometric imperfections.

General studies of this behavior for elastic structures have been made by Koiter [6] and Budiansky and Hutchinson [7]. For our study, we shall again assume that $\dot{y}_o = \dot{z}_o = 0$ and consider the following three cases.

(a) Elastic case ($\varkappa = 0$).

The effect of infinitesimal geometric imperfections for the problem of elastic shallow arches was first studied by Hoff and Bruce [1] with the use of the potential surface for the perfect arch. Their results are to be obtained here through consideration of the limiting behavior of an imperfect arch with vanishing imperfections.

When the imperfection z_o is small, so that $z_o^2 << y_o^2$, the critical points (y_e, z_e) can be determined by the following two simultaneous equations derived from Eqs. (20) and (21):

$$y_e - y_o + y_e\left(y_e^2 - y_o^2 + 4z_e^2\right) + r = 0 \quad , \tag{36a}$$

$$4\left(z_e - z_o\right) + z_e\left(y_e^2 - y_o^2 + 4z_e^2\right) = 0 \quad . \tag{36b}$$

Consider first that y_o is some fixed number and that z_o tends to zero. In the limit as z_o tends to zero, z_e either approaches zero or approaches a nonzero limit value. If z_e approaches zero, then Eq. (36a) reduces to Eq. (29). If z_e approaches a nonzero limit, however, then Eq. (36b) becomes

$$z_e \left(y_e^2 - y_o^2 + 4z_e^2 + 4 \right) = 0 \quad . \tag{37}$$

When $y_o \leq 2$, we see that the expression in parenthesis in Eq. (37) is positive. Equation (37) would then imply $z_e = 0$. Hence, the limit of z_e as z_o tends to zero can be different from zero only if $y_o > 2$.

Equations (36a, b) can be combined to give

$$z_e \left(3y_e + y_o - r \right) - 4y_e z_o = 0 \quad .$$

If the limit of z_e as z_o tends to zero is not zero, this equation gives in the limit

$$y_e = \frac{1}{3} (r - y_o) \quad , \quad y_o \geq 2 \tag{38}$$

and it then follows from Eq. (37) that

$$z_e = \pm \frac{1}{2} \left[y_o^2 - 4 - \frac{1}{9} (r - y_o)^2 \right]^{1/2} \quad , \quad y_o \geq 2 \quad . \tag{39}$$

Of the three critical points on the y-axis, two are local minima and one is a local maximum. We shall denote the local minima by M_1 and M_2, where M_1 is the minimum closest to the initial point. Equations (38) and (39) define two saddle points, symmetric about $z = 0$.

From Eq. (24), the potential energy for small z_o is

$$U = \frac{1}{2} \left(y - y_o \right)^2 + 8z^2 + \frac{1}{4} \left(y^2 - y_o^2 + 4z^2 \right)^2 + r \left(y - y_o \right). \tag{40}$$

The potential energy $U = U_e$ at the saddle points is found from

Eqs. (38), (39) and (40):

$$U_e = \frac{1}{6}\left[\left(r - 4y_o\right)^2 - 24\right] \quad , \quad y_o \geq 2 \quad . \tag{41}$$

Under small load, the trajectory of the motion on (y, z) plane would move in the neighborhood of M_1. The neighborhood of M_2 is not accessible until the load is increased sufficiently so that there will exist a trajectory leading to the neighborhood of M_2 and along which U is nonpositive. A necessary condition for the existence at such a trajectory is given by consideration of the saddle point on the potential surface. The considered trajectory is seen to be impossible unless r is large enough so that the saddle point value of U_e of Eq. (41) is nonpositive. Hence, the critical condition of Hoff and Bruce for snap-through is

$$U_e = 0 \quad , \tag{42}$$

at the saddle points, and the associated critical load is found to be r_{cm}:

$$r_{cm} = 4y_o - 2(6)^{1/2} \quad , \qquad y_o \geq 2.04 \tag{43}$$

When Eq. (43) is used to substitute for r in Eqs. (38) and (39), the coordinates of the saddle points at $r = r_{cm}$ are found to be

$$y_e = y_o - \frac{2}{3}(6)^{1/2} \tag{44a}$$

$$z_e = \pm \left[\frac{(6)^{1/2} y_o - 5}{3} \right]^{1/2} . \qquad (44b)$$

Equation (44b) shows that the saddle point does not exist if y_o is less than $(5/(6)^{1/2}) = 2.04$. At $y_o = 5/(6)^{1/2}$, Eqs. (44a, b) give $z_e = 0$, $y_e = 1/(6)^{1/2}$ at $r_{cm} = 8/(6)^{1/2}$. This point is also a root of Eq. (29). It is the critical point which corresponds to the local maximum of U, as is discussed in case (a) of Section 3. Moreover, the value of U at that local maximum is zero. Hence, at $y = 5/(6)^{1/2}$, we have $r_{cm} = r_{cp} = 8/(6)^{1/2}$, the value of r_{cp} being computed from Eq. (32).

Consequently, Eq. (43) holds only for $y_o > 2.04$. For $y_o \leq 2.04$, the critical load for the slightly imperfect arch is the same as that for the perfect arch; it is r_{cp} as given by Eq. (32).

In Fig. 7, the result of Eq. (43) is shown by one of the dotted lines. It is seen that, if r_{cm} is an accurate measure of critical load, then for $y_o > 2.04$ the critical loads drop considerably due to the effect of small antisymmetrical imperfections.

Since the above method of determining the critical load of an imperfect arch does not examine the actual motion of the structure, it does not enable one to assert that the trajectory will pass through the saddle point even if Eq. (42) is satisfied. Equation (42) is a necessary condition for snap-through, but it is not a sufficient condition.

In order to clarify this point, we have obtained solutions to Eqs. (17), (18) and (19) numerically by using very small values for the geometrical imperfection parameter z_o in the range 10^{-3} to 10^{-8}. The critical loads obtained from the numerical solution for $z_o = 10^{-4}$ and various y_o, as well as those from Eqs. (32) and (43), are shown in Table 1 and Fig. 6. It is found that the calculated r_c is in agreement with the predictions of Eq. (43) to within an error not exceeding a few percent.

These results confirm that it is impossible to produce snap-through if the load is lower than the value r_{cm} given by Eq. (43). Consequently, the result of Hoff and Bruce furnishes a lower bound and a good approximation to the critical load for elastic arches with small imperfections, as was implied in [2]. The following observations were made from the numerical results: (i) the arch may oscillate nonlinearly for a period of time before it snaps through; (ii) after snap-through, the arch may snap back to its original shape.

If, for a fixed $y_o > 2.04$, the calculated critical load r_c is sought for very small values of z_o, anomalous results may be obtained. Typical of such results are those shown in Table 2 for $y_o = 4.5$. Values of r_c appear to increase as z_o gets smaller. The reason for this is that the potential surface over which the

trajectory travels is very "flat". This follows because, for small z_o, $\frac{\partial U}{\partial z}$ at $z = z_o$ is $O(z_o)$. Hence, in the absence of damping, the arch can oscillate for very long periods before snap-through. If the calculations on the computer are not continued long enough for these very small values of z_o, then we run the risk of not discerning motions which are actually buckled motions, simply because they are not observed for long enough time.

(b) Viscoelastic case ($0 < \varkappa < \infty$)

Values of r_c obtained by numerical solution of Eqs. (17), (18) and (19) with $\varkappa = 0.1$ and $\varkappa = 0.2$ are shown in Fig. 7 by dotted lines for very small imperfections ($z_o = 10^{-4}$ was the value used) and by solid lines for zero imperfection. The closed-form expressions obtained for the perfect elastic arch (Eqs. (32) and (35)) are likewise represented by solid lines, while those for the infinitesimally imperfect elastic arch (Eq. (43) and Eq. (48) below) are represented by dotted lines. As was noted in (c) of Section 3, the limit $\varkappa = \infty$ gives the same results as for quasi-static loading of an elastic arch.

These curves show that for finite values of $\varkappa$, and for values of y_o above a certain lower limit, r_c drops markedly with the introduction of a small imperfection. The lower limit for y_o, which is 2.04 for the elastic arch, is seen to be higher for nonzero $\varkappa$.

Moreover, the curious behavior exhibited in Table 2 for the elastic arch with very small values of z_o is not shown for the viscoelastic arch; in the latter case, the limit value of r_c is approached continuously in the calculations as z_o goes to zero. (cf. also Fig. 8).

For values of y_o not much above the lower limit, the dotted curves for $\varkappa = 0.1$ and $\varkappa = 0.2$ in Fig. 7 are seen to merge rapidly into a calculated dotted curve for $\varkappa = \infty$ in Fig. 7. Other data for smaller values of $\varkappa$, not shown in the figure, exhibit the same behavior. The data for the elastic arch, however, follow close to the curve r_{cm} for all $y_o > 2.04$. The transition between these two types of behavior occurs at values of $\varkappa \leq 10^{-4}$, but computations are again difficult for this regime.

(c) Quasi-static case ($\varkappa = \infty$)

Fung and Kaplan ([5], pp. 14 and 15) considered in some detail the snap-through of shallow arches due to antisymmetric bifurcation in quasi-static loading if y_o is greater than $\frac{1}{2}(22)^{1/2} = 2.34$. To render the present paper reasonably complete, we shall derive their results from our equations following the approach given in [2].

For quasi-static equilibrium at a point (y_e, z_e), under a load r, Eqs. (20) and (21) must be satisfied and in addition the

potential energy U must obey the following stability condition there:

$$\frac{\partial^2 U}{\partial y^2}\ \frac{\partial^2 U}{\partial z^2} - \left(\frac{\partial^2 U}{\partial y\,\partial z}\right)^2 > 0 \quad . \tag{45}$$

For z_o vanishingly small, we find from Eq. (24), the following partial derivatives at points with $z = 0$:

$$U_{yy} \equiv \frac{\partial^2 U}{\partial y^2} = 1 + 3y^2 - y_o^2 \quad ,$$

$$U_{zz} \equiv \frac{\partial^2 U}{\partial z^2} = 4\left[y^2 - y_o^2 + 4\right] \quad ,$$

$$U_{zy} \equiv \frac{\partial^2 U}{\partial y\,\partial z} = 0 \quad .$$

The condition (45) can then be written as

$$\underbrace{\left(1 + 3y^2 - y_o^2\right)}_{U_{yy}}\ \underbrace{\left(y^2 - y_o^2 + 4\right)}_{U_{zz}} > 0 \quad . \tag{46}$$

If r is sufficiently small, so that $y_o - y_e$ is small, the inequality (46) is evidently satisfied. As r increases and y_e decreases, either U_{yy} or U_{zz} will become negative, indicating a loss of stability. The critical values of y_e are called y_{c1} and y_{c2}:

$$U_{yy} = 0: \qquad y_{c1} \equiv \left(\frac{y_o^2 - 1}{3}\right)^{1/2} \tag{47a}$$

$$U_{zz} = 0: \qquad y_{c2} \equiv \left(y_o^2 - 4\right)^{1/2} \quad . \tag{47b}$$

It is easily verified that at $y_o = \frac{1}{2}(22)^{1/2}$, we have $y_{c1} = y_{c2}$, and

that $y_{c2} \gtrless y_{c1}$ for $y_o \gtrless \frac{1}{2}(22)^{1/2}$. Consequently, the critical value of y_e is y_{c1} if $y_o < \frac{1}{2}(22)^{1/2}$, and it is y_{c2} if $y_o > \frac{1}{2}(22)^{1/2}$. The corresponding values of r, with z_o vanishingly small, are obtained by substitution of y_{c1} and y_{c2} for y into Eq. (29). There is then obtained:

$$r_{cs} = y_o + 2\left(\frac{y_o^2 - 1}{3}\right)^{1/2} \qquad y_o \leqq \frac{1}{2}(22)^{1/2} \quad , \tag{35}$$

$$r_{cs} = y_o + 3\left(y_o^2 - 4\right)^{1/2} \qquad y_o \geqq \frac{1}{2}(22)^{1/2} \quad . \tag{48}$$

The first equation above is identical to Eq. (35), which was derived on the basis of symmetrical buckling. Equation (48) is the result of Fung and Kaplan [5].

Quasi-static snap-through for this problem is summarized in Table 3. It may be inferred from these results that the appearance of the cross sections of the potential surface close to the y-axis is that of a valley for $y_o < \frac{1}{2}(22)^{1/2}$ which changes to a ridge near $y_e = y_{c2}$ if $y_o > \frac{1}{2}(22)^{1/2}$.

5. UPPER BOUND FOR ELASTIC ARCHES WITH INFINITESIMAL IMPERFECTION

In contrast to the results for the perfect elastic arch, for which an exact closed-form expression (r_{cp}, Eq. (32)) for the critical load can be determined for all values of y_o ($y_o > \frac{1}{2}(6)^{1/2}$) at which

snap-through can occur, the critical load for an infinitesimally imperfect arch cannot be represented in closed form for $y_o > 5/(6)^{1/2}$ It has been shown in the preceding section that r_{cm}, Eq. (43), is a lower bound and generally a good approximation to r_c for $y_o > 5/(6)^{1/2}$ An upper bound for r_c was proposed in [2], and a summary of the results obtained there is as follows.

For any $y_o > 5/(6)^{1/2}$ consider the load r_{cg} which causes the saddle points to disappear, i.e., the load which causes the z_e of Eq. (39) to vanish. It is found that this load is

$$r_{cg} = y_o + 3(y_o^2 - 4)^{1/2} \quad . \tag{49}$$

Equation (49) has the same right-hand side as Eq. (48), but the interpretation here is different. When the saddle points disappear, they coalesce with one of the critical points on the y-axis. For $y_o < \frac{1}{2}(22)^{1/2}$, this critical point is the local maximum, but for $y_o > \frac{1}{2}(22)^{1/2}$, the critical point is the first minimum M_1. When this occurs, M_1 is no longer a stable equilibrium point of the potential surface with y and z coordinates, and dynamic snap-through must eventually occur.

A critical condition will occur when either the potential U is zero at the local maximum or M_1 becomes unstable. The first condition is governed by r_{cp} and the second by r_{cg}. The upper bound

on r_c is determined by whichever of these two values, r_{cp} or r_{cg}, is the least for a given y_o.

These results, and the other results presented here on dynamic buckling of an infinitesimally imperfect elastic shallow arch, can be summarized as follows:

$$
\begin{array}{ll}
y_o \leqq 1.224 & \text{no snap-through} \\
1.224 < y_o \leqq 2.04 & r_c = r_{cp} \\
2.04 < y_o \leqq 3.19 & r_{cm} \leqq r_c \leqq r_{cp} \\
3.19 > y_o & r_{cm} \leqq r_c \leqq r_{cg}
\end{array}
\tag{50}
$$

A comparison between this upper bound and the calculated values of r_c is shown in Table 1 and graphically in Fig. 6. The upper bound is considerably larger than r_c. The results of the present investigation, as discussed above in part (b) of Section 4, place a new interpretation on this upper bound, however. It is now seen that the upper bound values for r_c in (50) may be those actually approached by some arches with very small viscosity ($\varkappa = 0^+$) while the lower bound values for r_c in (50) are those actually approached for elastic or zero viscosity ($\varkappa = 0$) arches. In both cases we must consider that the arches are slightly imperfect ($z_o = 0^+$).

6. ARCHES WITH FINITE GEOMETRICAL IMPERFECTION ($z_o > 0^+$)

For the case of finite geometrical imperfections, the critical loads can be found from the numerical solution of Eqs. (17), (18) and (19). The critical loads for $z_o = 0.25$ and $\dot{z}_o = 0$ are shown as dotted curves in Fig. 5. The critical loads for the $\varkappa = \infty$ curve are obtained from the maximum point of the $r - y_e$ curve evaluated from Eq. (22).

As compared with the case of the perfect arch, the critical load is reduced considerably due to the imperfections. The reduction increases with the value of y_o. The effect of finite imperfections for various values of y_o is shown in Fig. 8. As expected, the critical load decreases as the value of initial imperfection increases. In accord with our previous discussion, a discontinuity in the critical load is found at $z_o = 0$ for the cases $y_o = 3$ and 4 but not for $y_o = 2$.

7. PRINCIPAL CONCLUSIONS

In summary, we have observed several types of discontinuous behavior of the calculated snap-through load r_c as a function of the imperfection amplitude z_o and the viscosity parameter $\varkappa$. This behavior depends also upon the rise y_o, as is discussed throughout the text, but in order to focus on the essential results, we will discuss the function $r_c(z_o, \varkappa)$ within the range of y_o upon which we calculated.

a) The introduction of an "infinitesimal" imperfection causes a jump or discontinuous drop in r_c: $r_c(0^+, \varkappa) < r_c(0, \varkappa)$ for $\varkappa \geq 0$. Larger imperfections lower r_c continuously (Fig. 8).

b) The critical loads $r_c(0^+, 0)$ were found to be close to but slightly above the Hoff and Bruce value (Eq. (43)) for the elastic arch (see Table 1 and Fig. 6).

c) The critical loads $r_c(0^+, 0^+)$ were found to be between the upper bound loads (Eq. (50)) by Simitses and the lower bound loads (Eq. (43)) by Hoff and Bruce. A rapid increase of the critical load is observed by introducing very small viscosity, i. e., $r_c(0^+, 0^+) > r_c(0^+, 0)$, (see Fig. 6).

d) For finite values of $\varkappa$ and z_o (Fig. 7), r_c increases with increasing $\varkappa$ to a maximum value determined by the quasi-static snap-through load.

e) Computation of r_c for both z_o and $\varkappa$ extremely small can lead to anomalous results for r_c because the arch can oscillate for a long time before snap-through.

A related problem of dynamic buckling of sinusoidal, simply-supported shallow arches has been considered by Lock [8]. In his analysis, Lock considers what is called in the present paper the

perfect arch, that is $z_o = 0$, but he includes infinitesimal initial antisymmetric velocity disturbances, that is $\dot{z}_o$ of the order of 5×10^{-3}, which are not considered here. These antisymmetric initial velocity components serve in Lock's investigation to produce antisymmetric snap-through. Moreover, in Lock's analysis, energy dissipation is introduced by external damping rather than by material viscosity as is done in the present paper.

Since the conditions of imperfection, load application and damping used in Lock's work and the present work are different, there is no reason to expect the same conclusions. The following points can be made in comparison of his results and our results:

(1) In the elastic case, Lock finds that the dynamic buckling load r_c has a discontinuous jump at $y_o = 4.375$. For $y_o > 4.375$, the value of r_c can be higher than the quasi-static buckling load r_{cg}. This behavior is not seen in the present case for $y_o \leq 4.5$.

(2) In the case of small damping, Lock finds that the buckling load for $y_o \geq 4.0$ is essentially the quasi-static buckling load. The same result is also observed in our calculation (see Fig. 6).

Acknowledgment

The authors wish to express their thanks to Mr. W. N. Huang for his assistance in computation and preparation of figures and to Mrs. Anne Brick for typing the manuscript.

References

1. N. J. Hoff and V. G. Bruce, "Dynamic Analysis of the Buckling of Laterally Loaded Flat Arches," J. Math. Physics, Vol. 32, 1954, pp. 276-288.

2. G. J. Simitses, "Dynamic Snap-through Buckling of Low Arches and Shallow Spherical Caps," Ph. D. Dissertation, Department of Aeronautics and Astronautics, Stanford University, June 1965.

3. W. Nachbar and N. C. Huang, "Dynamic Snap-through of a Simple Viscoelastic Truss," Quart. Appl. Math., Vol. 25, 1967.

4. A. Ralston and H. Wilf, Mathematical Methods for Digital Computers, John Wiley and Sons, Inc., New York, 1960, p. 110.

5. Y. C. Fung and A. Kaplan, "Buckling of Low Arches or Curved Beams of Small Curvature," NACA Technical Note 2840, November 1952.

6. W. T. Koiter, "Elastic Stability and Post-buckling Behavior," Nonlinear Problems, edited by R. E. Langer, The University of Wisconsin Press, Madison, Wisconsin, 1963, p. 257.

7. B. Budiansky and J. W. Hutchinson, "Dynamic Buckling of Imperfection-sensitive Structures," Proceedings of the Eleventh International Congress of Applied Mechanics, Munich, 1964, Edited by H. Görtler, Springer-Verlag, New York, p. 636.

8. M. H. Lock, "Snapping of a Shallow Sinusoidal Arch under a Step Pressure Load," AIAA Journal, Vol. 4, 1966, pp. 1249-1256.

y_o	2.23	2.50	2.71	3.00	3.24	3.50	3.71	4.00	4.25	4.50
r_{cp} or r_{cg} [Eq. (32) or (49)]	4.09	5.52	6.82	9.05	10.86	12.12	13.07	14.41	15.50	16.59
r_c	4.04	5.39	5.96	7.13	8.13	9.19	10.06	11.19	12.31	13.79
r_{cm} [Eq. (43)]	4.02	5.10	5.94	7.10	8.06	9.10	9.94	11.10	12.10	13.10

TABLE 1. Comparison of the Calculated Values of Critical Loads with the Upper and Lower Bounds for Elastic Arches with $z_o = 10^{-4}$.

z_o	10^{-3}	10^{-4}	10^{-5}	10^{-6}
r_c	13.61	13.79	14.45	16.65*

TABLE 2. Effect of an Infinitesimal Imperfection on the Critical Load for the Elastic Arch with $y_o = 4.5$.

* This value of r_c is higher than the upper bound value $r_{cg} = 16.59$ (Table 1). For extremely small values of z_o, the arch may snap-through after a long time of oscillation. The critical value may decrease considerably if the overall machine calculating time is allowed to increase.

Range of y_o	Critical value of y_e	Stability condition $U_{yy}U_{zz} > 0$	y_e at snap-through	r_{cs} Snap-through load
$y_o < 1$	y_{c1} and y_{c2} nonexistent.	U_{yy} and U_{zz} positive for all y_e.	No snap-through.	—
$1 < y_o < 2$	y_{c2} nonexistent $y_{c1} > 0$.	U_{zz} positive for all y_e. U_{yy} positive for $y_e > y_{c1}$, and $U_{yy} = 0$ for $y_e = y_{c1}$.	Symmetric snap-through at $y_e = y_{c1}$.	Eq. (35)
$2 < y_o < \frac{1}{2}(22)^{1/2}$	$y_{c1} > y_{c2}$	U_{zz} positive for all $y_e \geq y_{c1}$. U_{yy} positive for $y_e > y_{c1}$, and $U_{yy} = 0$ for $y_e = y_{c1}$.	Symmetric snap-through at $y_e = y_{c1}$	Eq. (35)
$y_o > \frac{1}{2}(22)^{1/2}$	$y_{c2} > y_{c1}$	U_{yy} positive for all $y_e \geq y_{c2}$. U_{zz} positive for $y_e > y_{c2}$, and $U_{zz} = 0$ for $y_e = y_{c2}$.	Unsymmetric snap-through at $y_e = y_{c2}$.	Eq. (48)

TABLE 3. Summary of Results on Quasi-Static Snap-Through.

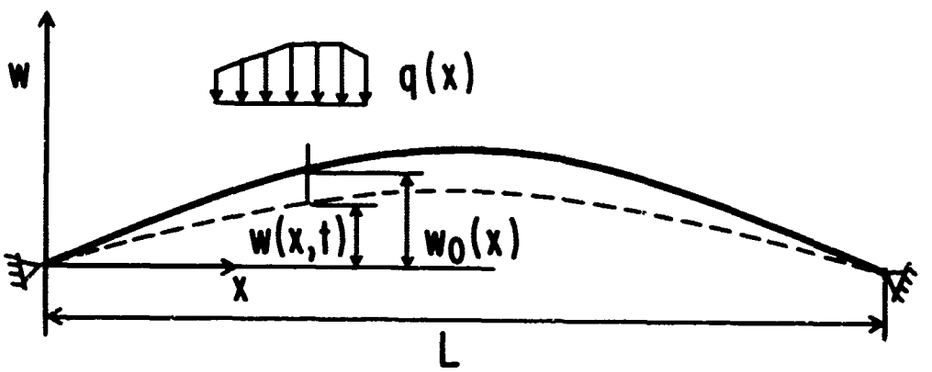

Fig. 1. Geometry of the Arch.

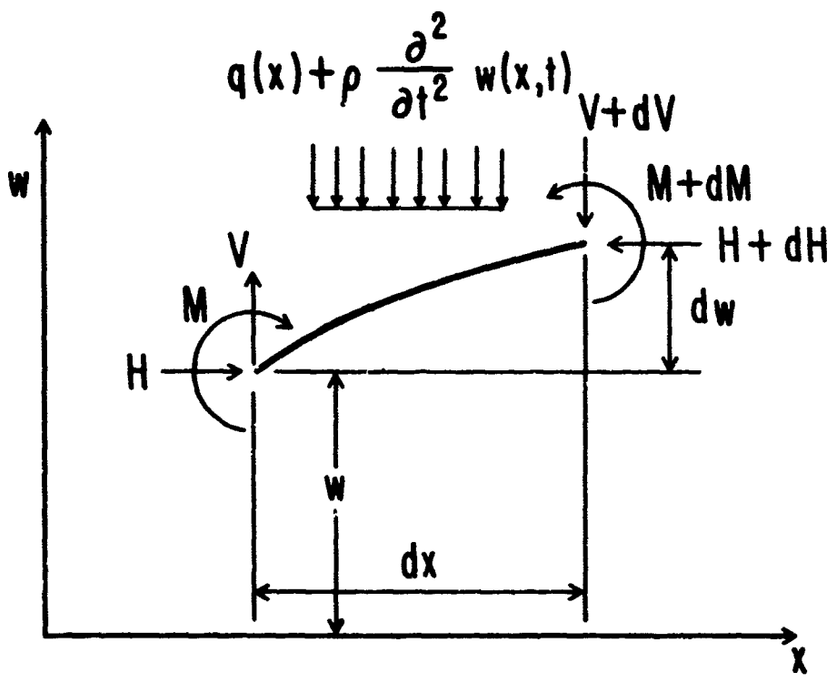

Fig. 2. Forces and Moments in the Arch.

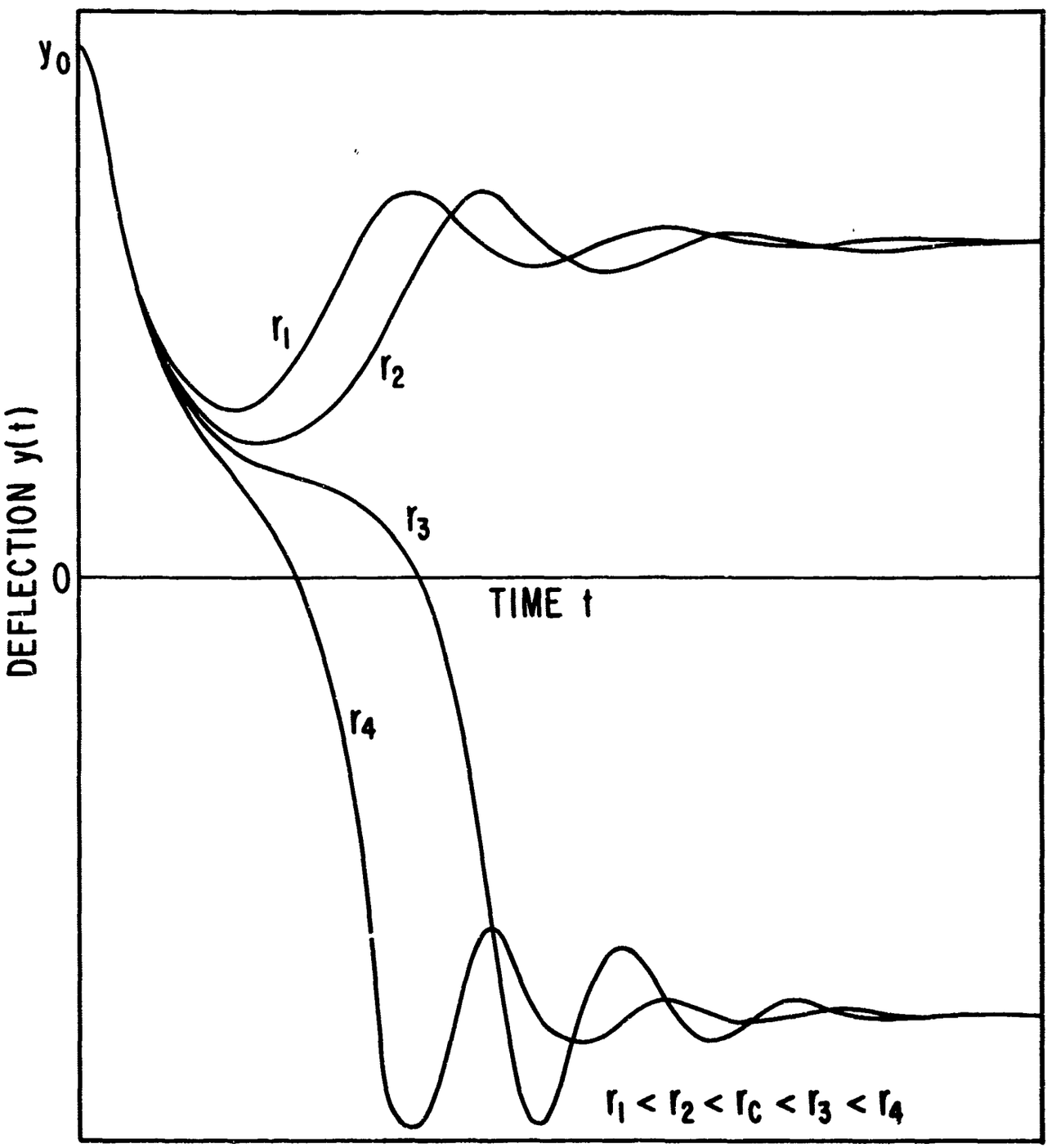

Fig. 3. Symmetric Deformations Under Various Loads.

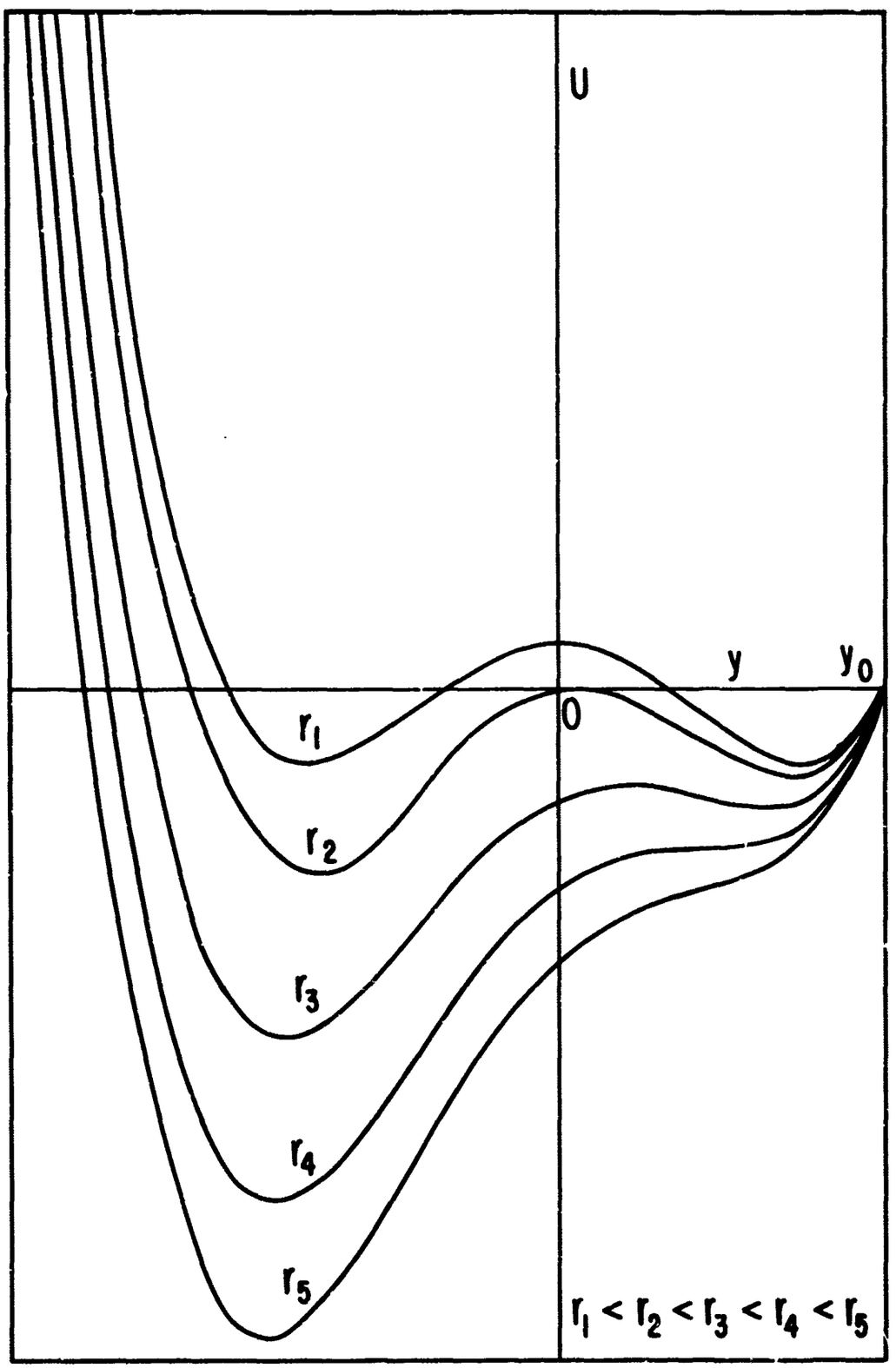

Fig. 4. Potential Curves.

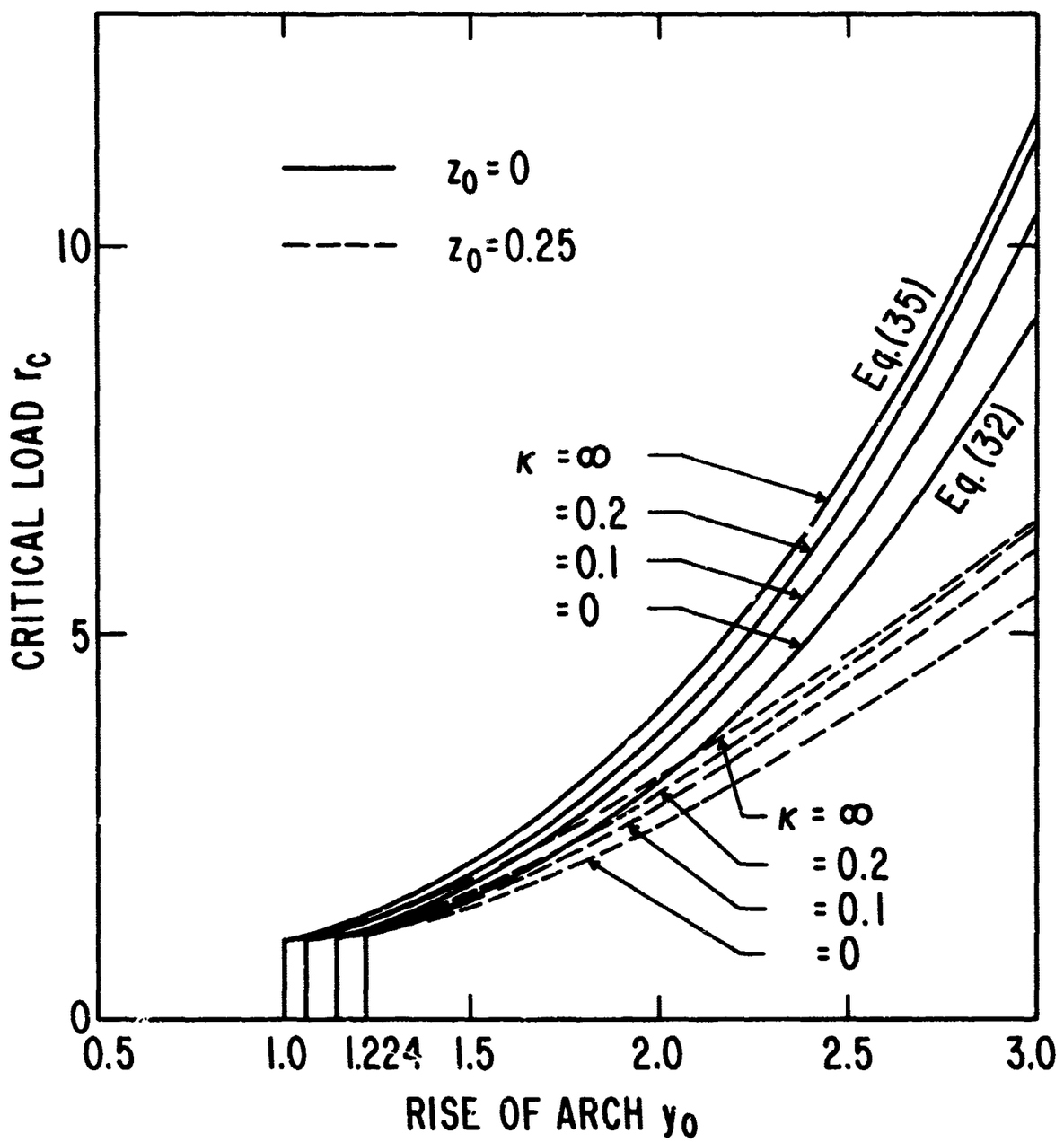

Fig. 5. Critical Loads for Shallow Arches with Imperfections $z_o = 0$ and $z_o = 0.25$.

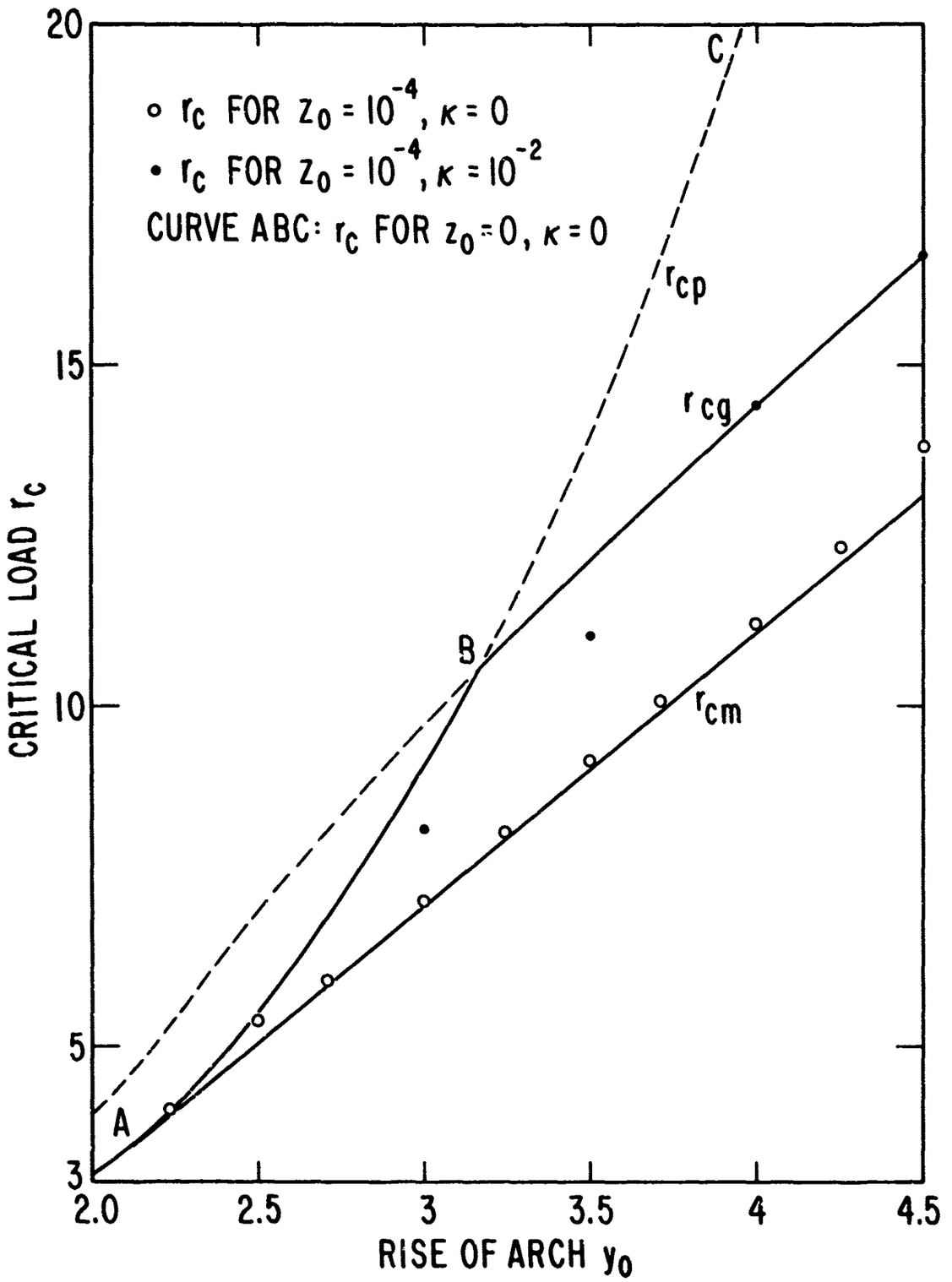

Fig. 6. Upper and Lower Bounds on r_c of Elastic Arches: Comparison with Calculations for Slightly Imperfect, Slightly Viscoelastic Arches.

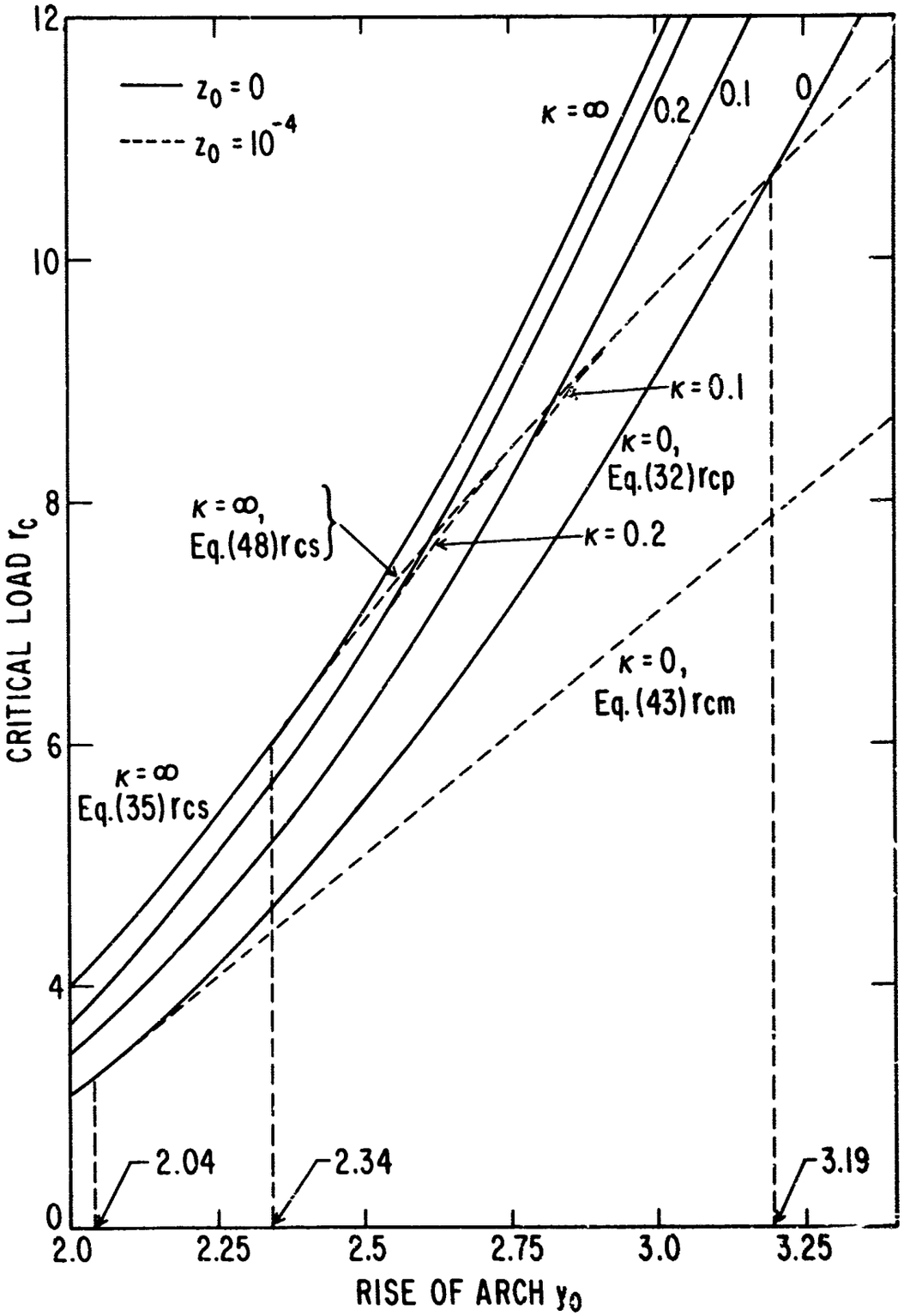

Fig. 7. Effect of Infinitesimal Initial Geometric Imperfection.

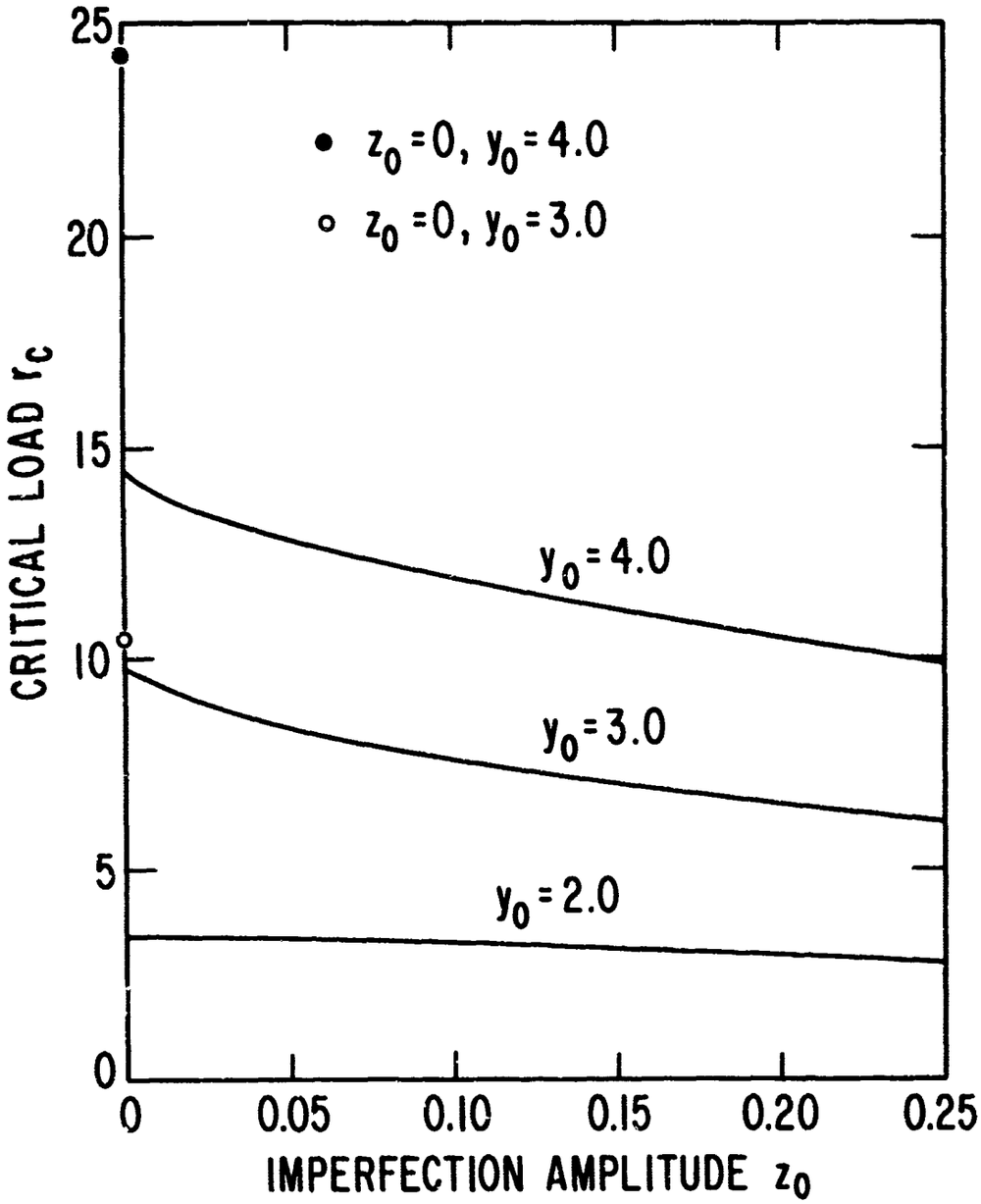

Fig. 8. Effect of Finite Initial Geometric Imperfection ($\varkappa$ = 0.1).

Unclassified

Security Classification

DOCUMENT CONTROL DATA - R&D

(Security classification of title, body of abstract and indexing annotation must be entered when the overall report is classified)

1. ORIGINATING ACTIVITY *(Corporate author)*
University of California, San Diego
Dept. of Aerospace & Mechanical Engineering Sciences
La Jolla, California 92037

2a. REPORT SECURITY CLASSIFICATION
Unclassified

2b. GROUP

3. REPORT TITLE
DYNAMIC SNAP-THROUGH OF IMPERFECT VISCOELASTIC SHALLOW ARCHES

4. DESCRIPTIVE NOTES *(Type of report and inclusive dates)*
Scientific Interim

5. AUTHOR(S) *(Last name, first name, initial)*
N. C. Huang and W. Nachbar

6. REPORT DATE	7a. TOTAL NO. OF PAGES	7b. NO. OF REFS
March 1967	43	8

8a. CONTRACT OR GRANT NO.	9a. ORIGINATOR'S REPORT NUMBER(S)
AF-AFOSR 1226-67	No. 1
b. PROJECT NO. 9782-01	
c. 61445014	9b. OTHER REPORT NO(S) *(Any other numbers that may be assigned this report)*
d. 681307	AFOSR 67-0856

10. AVAILABILITY/LIMITATION NOTICES
Distribution of this document is unlimited

11. SUPPLEMENTARY NOTES	12. SPONSORING MILITARY ACTIVITY
TECH., OTHER	AF Office of Scientific Research (SREM) 1400 Wilson Boulevard Arlington, Virginia 22209

13. ABSTRACT

Dynamic snap-through or dynamic buckling of imperfect viscoelastic shallow arches with hinged ends is considered under step loads of infinite duration. Attention is principally devoted to the influence both of small imperfections and of small amounts of damping, acting together, on the critical loads. For the problem considered, the Voigt model is used for viscoelasticity, the deflection is represented by the first two harmonic modes, and imperfections have the shape of the second (antisymmetric) mode. Results obtained by numerical integration of the differential equations show that the critical load exhibits a jump discontinuity in the limit both for vanishing imperfection and for vanishing viscosity. Critical loads for slight imperfect and elastic (inviscid) arches are slightly higher than those from the saddle point formula of Hoff and Bruce (J. Math. Physics, 32, 1954, 276), confirming that the formula gives a lower bound on the critical load. However, critical loads for arches with slight imperfection and slight viscosity are considerably higher than for the elastic arches. Another closed-form expression is shown to be in good agreement with these results. For finite amounts of viscosity, the critical loads tend rapidly to the values obtained for infinite viscosity, which are the same as the critical loads for quasi-static buckling. Apart from the jump discontinuity at zero, the critical load for any viscosity decreases continuously and monotonically with imperfection.

DD FORM 1 JAN 64 1473 0101-807-6800

Unclassified

Security Classification

Unclassified

Security Classification

14. KEY WORDS	LINK A		LINK B		LINK C	
	ROLE	WT	ROLE	WT	ROLE	WT
Dynamic buckling, Dynamic buckling of viscoelastic structures, Dynamic snap-through of viscoelastic structures, Arches, Stability of Arches, Viscoelastic Stability of Structures with imperfections.						

INSTRUCTIONS

1. ORIGINATING ACTIVITY: Enter the name and address of the contractor, subcontractor, grantee, Department of Defense activity or other organization *(corporate author)* issuing the report.

2a. REPORT SECURITY CLASSIFICATION: Enter the overall security classification of the report. Indicate whether "Restricted Data" is included. Marking is to be in accordance with appropriate security regulations.

2b. GROUP: Automatic downgrading is specified in DoD Directive 5200.10 and Armed Forces Industrial Manual. Enter the group number. Also, when applicable, show that optional markings have been used for Group 3 and Group 4 as authorized.

3. REPORT TITLE: Enter the complete report title in all capital letters. Titles in all cases should be unclassified. If a meaningful title cannot be selected without classification, show title classification in all capitals in parenthesis immediately following the title.

4. DESCRIPTIVE NOTES: If appropriate, enter the type of report, e.g., interim, progress, summary, annual, or final. Give the inclusive dates when a specific reporting period is covered.

5. AUTHOR(S): Enter the name(s) of author(s) as shown on or in the report. Enter last name, first name, middle initial. If military, show rank and branch of service. The name of the principal author is an absolute minimum requirement.

6. REPORT DATE: Enter the date of the report as day, month, year, or month, year. If more than one date appears on the report, use date of publication.

7a. TOTAL NUMBER OF PAGES: The total page count should follow normal pagination procedures, i.e., enter the number of pages containing information.

7b. NUMBER OF REFERENCES: Enter the total number of references cited in the report.

8a. CONTRACT OR GRANT NUMBER: If appropriate, enter the applicable number of the contract or grant under which the report was written.

8b, 8c, & 8d. PROJECT NUMBER: Enter the appropriate military department identification, such as project number, subproject number, system numbers, task number, etc.

9a. ORIGINATOR'S REPORT NUMBER(S): Enter the official report number by which the document will be identified and controlled by the originating activity. This number must be unique to this report.

9b. OTHER REPORT NUMBER(S): If the report has been assigned any other report numbers *(either by the originator or by the sponsor)*, also enter this number(s).

10. AVAILABILITY/LIMITATION NOTICES: Enter any limitations on further dissemination of the report, other than those imposed by security classification, using standard statements such as:

(1) "Qualified requesters may obtain copies of this report from DDC."

(2) "Foreign announcement and dissemination of this report by DDC is not authorized."

(3) "U. S. Government agencies may obtain copies of this report directly from DDC. Other qualified DDC users shall request through

_____."

(4) "U. S. military agencies may obtain copies of this report directly from DDC. Other qualified users shall request through

_____."

(5) "All distribution of this report is controlled. Qualified DDC users shall request through

_____."

If the report has been furnished to the Office of Technical Services, Department of Commerce, for sale to the public, indicate this fact and enter the price, if known.

11. SUPPLEMENTARY NOTES: Use for additional explanatory notes.

12. SPONSORING MILITARY ACTIVITY: Enter the name of the departmental project office or laboratory sponsoring *(paying for)* the research and development. Include address.

13. ABSTRACT: Enter an abstract giving a brief and factual summary of the document indicative of the report, even though it may also appear elsewhere in the body of the technical report. If additional space is required, a continuation sheet shall be attached.

It is highly desirable that the abstract of classified reports be unclassified. Each paragraph of the abstract shall end with an indication of the military security classification of the information in the paragraph, represented as *(TS), (S), (C), or (U)*.

There is no limitation on the length of the abstract. However, the suggested length is from 150 to 225 words.

14. KEY WORDS: Key words are technically meaningful terms or short phrases that characterize a report and may be used as index entries for cataloging the report. Key words must be selected so that no security classification is required. Identifiers, such as equipment model designation, trade name, military project code name, geographic location, may be used as key words but will be followed by an indication of technical context. The assignment of links, roles, and weights is optional.

Unclassified

Security Classification